

**Variability Of Latent Heat Flux
Over The Indian Ocean**

A Dissertation for

Course Code Course Title: MSC 617 Discipline Specific Dissertation

Credits: 16

Submitted in partial fulfillment of Master's Degree

M.Sc. In Marine Sciences

By

Srushti Milind Meshram

Roll Number: 22P0400025

ABC ID: 538027993367

PR Number: 202200081

Under the Supervision of

Nikita Mangeshkar

School of Earth, Ocean and Atmospheric Sciences
Marine Sciences



GOA UNIVERSITY

April 2024



Seal of the

Examined by:
School

DECLARATION BY STUDENT

I hereby declare that the data presented in this Dissertation entitled "**Variability Of Latent Heat Flux Over The Indian Ocean**" is based on the results of investigations carried out by me in the Discipline of **Marine Sciences** at the School of Earth, Ocean and Atmospheric Sciences, Goa University under the Supervision of Dr. Nikita Mangeshkar and the same has not been submitted elsewhere for the award of a degree or diploma by me. Further, I understand that Goa University or its authorities will be not be responsible for the correctness of observations / experimental or other findings given in the dissertation.

I hereby authorize the University authorities to upload this dissertation on the dissertation repository or anywhere else as the UGC regulations demand and make it available to any one as needed.



Srushti Milind Meshram

Seat No.: : 22P0400025

Date:- 02/05/2024
Place:- Goa University , Taleigao Plateau, Goa

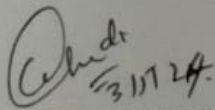
COMPLETION CERTIFICATE

This is to certify that the dissertation report "**Variability Of Latent Heat Flux Over The Indian Ocean**" is a bonafide work carried out by Ms. Srushti Milind Meshram under my supervision in partial fulfillment of the requirements for the award of the degree of Master of Science in the Discipline of Marine Sciences at the School of Earth, Ocean and Atmospheric Sciences, Goa University



Nikita Mangeshkar
Discipline of Marine Sciences,
School of Earth, Ocean and Atmospheric Sciences

Date: 02/05/24



Sr. Prof. Sanjeev C. Ghadi,
Senior Professor and Dean
Marine Sciences
School of Earth, Ocean and Atmospheric Sciences Date:
Place: Goa University, Taleigão Plateau, Goa



School Stamp

chapter	Particulars	Page numbers
		iv
		v
		vii
		viii
		ix
		x
1	Introduction	1
1.1	Background	1
1.2	Aims and Objective	14
1.3	Scope	
2	Literature Review	
3	Data Methodology	
4	Observations	
5	Discussion	
6	Conclusion	
7	References	

PREFACE

Indian Ocean its name from India, it differs from the Atlantic and Pacific in the fact that, in the Northern Hemisphere, it is landlocked and does not reach Arctic waters, thus lacking a temperate- to-cold zone in this area. The Indian Ocean is the third largest of the world's five oceans (after the Pacific Ocean and Atlantic Ocean, but larger than the Southern Ocean and Arctic Ocean). Four critically important access waterways are the Suez Canal (Egypt), Bab el Mandeb (Djibouti-Yemen), Strait of Hormuz (Iran-Oman), and Strait of Malacca (Indonesia-Malaysia). The decision by the International Hydrographic Organization in the spring of 2000 to delimit a fifth ocean, the Southern Ocean, removed the portion of the Indian Ocean south of 60 degrees south latitude. Among its many physical parameters Sea Surface Temperature (SST), Sea Level Pressure and Latent Heat Flux an essential physical parameter in the ocean's complex web of life. The Indian Ocean basin is **the warmest ocean basin on the planet**. Temperatures vary according to location and the ocean's currents. In coastal regions near the Equator, the temperature can reach 28°C (82°F). South of 20° S surface temperatures decrease at a constant rate with increasing latitude, from 22° to 24 °C (72 to 75 °F) down to near freezing at 60° S.

Understanding the variability of Sea Surface Temperature, Pressure and Latent Heat Flux concentration is not merely an academic pursuit; it has profound implications on our understanding of Temperature Variation, Climate change, and Pressure. Changes in Surface Temperature and Latent Heat Flux levels can influence the entire parameters from pelagic to benthic along with complete ecosystem, and can serve as early indicators of environmental shifts that may have far-reaching consequences for both marine life and human societies that depend on the ocean for sustenance and livelihood. In the current era of climate change, it is important to understand the variability of SST, Latent Heat Flux, and Pressure variations. This encouraged me to study on the topic “**Variability of Latent Heat Flux over The Indian Ocean.**”

ACKNOWLEDGEMENTS

I would like to express my heartfelt gratitude to the God for granting me the strength throughout the journey of completing this dissertation. I extend my deepest appreciation to my family for their support.

A special word of thanks goes to my guide Ms. Nikita Mangeshkar, Assistant Professor, at the School of Earth, Ocean and Atmospheric Sciences, Goa University, for her invaluable support and guidance throughout the dissertation process. Her expertise, patience, and encouragement have been instrumental in shaping this work and navigating through its complexities.

I would like to thank Sr. Prof. Sanjeev C. Ghadi, Dean of School of Earth, Ocean and Atmospheric Sciences, Goa University and Sr. Prof. C. U. Rivonker, Former Dean of School of Earth, Ocean and Atmospheric Sciences, for providing with the necessary facilities that aided in the completion of my dissertation work.

Additionally, I would like to thank the data providers –The data is of Net Heat Flux, Pressure of Indian Ocean, and Sea Surface Temperature from ERA5. The data was downloaded from the webpage:

[https://cds.climate.copernicus.eu/cdsapp#!/dataset/reanalysis-era5-single-levels-monthly-means?
tab=form](https://cds.climate.copernicus.eu/cdsapp#!/dataset/reanalysis-era5-single-levels-monthly-means?tab=form)

I would also like to extend my heartfelt appreciation to my dear friend Mr. Pavas Mani for his assistance and support. His willingness to lend a helping hand, offer insightful advice, is deeply appreciated. To everyone who has played a part, no matter how big or small, in this journey, I offer my sincere gratitude.

LIST OF ABBREVIATIONS

Entity	Abbreviation
Sea Surface Temperature	SST
North	N
Latent Heat Flux	LHF
Tropical Indian OceanI	TIO
Bay Of Bengal	BOB
South Eastern	SE
South Western	SW

LIST OF FIGURES

Figure Number	Description	Page Number
1.1	The seasonal evolution and interannual variability of latent heat flux (LHF) over the tropical Indian Ocean (TIO) region is examined for the period January - December. The seasonal distribution of LHF is dominated by the winter pattern of each hemisphere in the TIO	13
3.1	Area of Study entire Indian Ocean (-30°N to 30°N Latitude), (40°E to 120°W longitudes)	24
4.1	Pressure concentration map (Pascals) in the Indian Ocean (-30 °N to 30 °N, 40 °E to 120 °W), averaged in the period from January 2023 to December 2023. (Climatologically)	41
4.2	Latent Heat Flux concentration map in the Indian Ocean (-30 °N to 30 °N, 40 °E to 120 °W), averaged in the period from January 2023 to December 2023. (Climatologically)	45
4.3	Sea Surface Temperature (SST) concentration map (Degree Celcius) in the Indian Ocean (-30 °N to 30 °N, 40 °E to 120 °W), averaged in the period from January 2023 to December 2023. (Climatologically)	46
4.4	Sea Surface Temperature (SST) concentration map (Degree Celcius) in the Indian Ocean (-30 °N to 30 °N, 40 °E to 120 °W), averaged in the period from January 2023 to December 2023.	47

ABSTRACT

Sea Surface Temperature (SST) data was used from Copernicus era5 with resolution 0.25×0.25 from the period 2023 January to December for the Entire Indian Ocean -30 to 30 and 40 to 120 . The data was averaged and plotted in Time Series and Spatial Plot. Similarly the Oceanic Pressure data was taken from APDRC. The data was averaged and images were obtained showing the region (Indian Ocean) with variability in the Sea Surface Temperature, Latent Heat Flux and Oceanic Pressure. The Basin -30 N to 30 E and 40 E to 120 W is 26.3 degree Celsius which fluctuates month wise. Similarly, the Pressure mainly lower in the entire Indian Ocean that ranges between 100.0 to 103.5 Pascal. Simultaneously, the Latent Heat Flux ranges -1.50 to 0.00 w/m².

INTRODUCTION

1. Background

The Indian Ocean stands as the third largest ocean in the world, this covering approximately 70.56 million square kilometres. Indian Ocean is known for its rich biodiversity, marine life, and important trade routes that connect countries across Asia, Africa and Australia. The Indian Ocean is also significant for its role in shaping the climate of the surrounding regions. Air-sea heat fluxes are fundamental processes that influence the interactions between the ocean and atmosphere in the Earth system. This fluxes involve the transfer of heat, moisture, and momentum between the air and sea through various mechanisms such as radiation, conduction, and convection. Air-sea heat fluxes are a part of the complex system that maintains the Earth's climate balance by allowing the ocean and atmosphere to exchange energy. This exchange to energy affects the temperature, humidity, and wind patterns, which in turn influence the global climate, weather patterns, and ocean currents (Taylor et al 2023). On the year 2023, the Indian Ocean exhibits a complex pattern of seasonal ocean circulation, which is influenced by several factors such as monsoon, winds, and ocean currents.

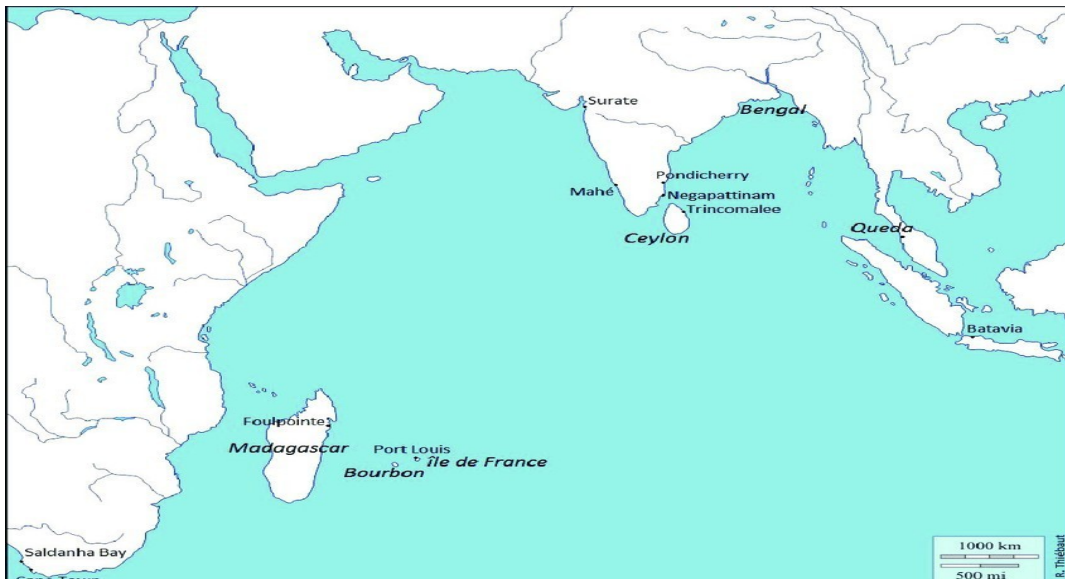


Fig. 1.1 Area of the Study (Indian Ocean) Source - NOAA

Figure 1.1 The seasonal evolution and interannual variability of latent heat flux (LHF) over the tropical Indian Ocean (TIO) region is examined for the period 1980–2019. The seasonal distribution of LHF is dominated by the winter pattern of each hemisphere in the TIO.

Climatologically high LHF is mostly confined to the Arabian Sea and Bay of Bengal regions in the north Indian Ocean and the tonal belt between 10°S and 25°S in the south Indian Ocean. Warm and cold phases of El-Niño Southern Oscillation, Indian Ocean Dipole (IOD), and their co-occurrence events leave distinct LHF signatures over the TIO. The LHF anomalies during these events are more profound than pure events with enhanced latent heat loss when the La Niña and negative IOD events coincide. The LHF anomalies associated with the wind-evaporation-SST feedback is prominent when positive IOD co-occur with the El-Niño event. Both the vertical humidity gradient and wind speed changes play substantial roles in driving LHF anomalies during the co-occurring events of NIOD and La Niña.

The global annual mean of latent heat flux (LHF) export is equivalent to 23% of the incoming solar radiation at the top of the atmosphere (Trenberth et al., 2009). The LHF plays a central role in ocean–atmosphere coupling and the thermodynamic feedback between atmosphere and ocean. The LHF loss from the ocean balances a significant portion of the net surface radioactive heat gain (da Silva et al., 1994).

Two different surface water masses are formed in the northern Indian Ocean, the high-salinity water of the Arabian Sea and the low-salinity water of the Bay of Bengal; these are caused by the excess of either evaporation or precipitation, which is intensified by the large runoff into the Bay of Bengal. The low-salinity water of the Bay of Bengal flows during the NE monsoon south of Ceylon to the west, with one branch continuing westward along 5°N,

and the other north west ward along the coast of India. During the SW monsoon it flows to

the SE along the coast of Sumatra where its salinity is further reduced by the high rainfall in this region. This low-salinity tropical surface water then flows westward in the northern portions of the South Equatorial Current, and can be followed near 10° S as a surface-salinity minimum extending all the way to Africa. The salinity of this water is kept low by the strong rainfall in the Inter tropical Convergence Zone during the NE monsoon season. In recent years, LHF has been a topic of active research because of its crucial role in modulating the upper oceanic heat budget in tropics. (e.g., Girishkumar et al., 2017; Joseph et al., 2021; Mathew et al., 2020). Using the moored buoy data analysis, Zhang and McPhaden (1995) found that in the equatorial Pacific, the background SST itself has influence on the relationship between SST change and LHF change, indicating that the thermodynamic components alone cannot explain LHF variability. They have shown that at low SSTs, vertical humidity gradient primarily determines the LHF, and at high SST, windspeed changes determine the variations in LHF. Based on the analysis of satellite remote sensing data and reanalysis products, Nisha et al. (2012) reached a similar conclusion for the northern Indian Ocean basin. Based on reanalysis products, Kumar et al. (2017) concluded that the LHF variability of north Indian Ocean is largely controlled by air-sea temperature and humidity components. Mathew et al. (2020) showed that the intense release of LHF over the northern BoB associated with the warming phase of intra-seasonal oscillation during southwest monsoon is facilitated by the high sensitivity of surface saturation specific humidity to variations in SST. Sea Surface Temperature (SST) through analysis of their perspective datasets. The objective is to conduct a thorough investigation of the spatial and temporal variations in latent heat flux on the different months of the year to determine how LHF

changes over time.

Latent heat flux (LHF) and sensible heat flux (SHF) are two essential components of the exchange of heat and moisture between the atmosphere and the ocean, Both LHF and SHF are important for the ocean's salinity budget of the upper ocean (Jury and Walker, 1988; Lee-Thorp et al., 1998; Rouault et al., 2000).

1. AIM AND

OBJECTIVES AIM

The aim of this dissertation work is to study the variability of Latent Heat Flux over the Indian Ocean and the concentration in the Indian Ocean ranges from January to December 2023.

OBJECTIVES

To study the average monthly, seasonal and annual variability of Sea Surface Temperature, Total Pressure and Latent Heat Flux in the Indian Ocean.

To study the trends in the monthly, seasonal and annual variability of the Heat Flux Concentration in the Indian Ocean.

2. SCOPE

The scope of this study is to study the variability of Latent Heat Flux concentration in the Indian Ocean using a freely-available online dataset of monthly Sea Surface Temperature, Total Pressure and Latent Heat Flux.

The study will include computing averages and the slopes of trend lines of Sea Surface Temperature (SST), Total Pressure, Latent Heat Flux. This is done at monthly, seasonal and for the entire time-period studied. However, the factor of the variability will not be studied.

CHAPTER 2: LITERATURE REVIEW

The changes in the thermal conditions over the TIO are mainly contributed by changes in the LHF. In a warm-ing climate, the near-surface humidity (Q_a) has a significant role in modulating the rate of LHF transfer (Held & Soden, 2006; Kumar et al., 2017). The amount of water vapour in the air needs to be lower than surface saturation humidity (Q_s) for evaporation to take place. Surface winds directly maintain a vertical air-sea humidity gradient by carrying the water vapour away from evaporating sea surface.

Previous studies have decomposed the LHF change into oceanic response and atmospheric forcing to investigate the role of surface heat flux adjustments in TIO warming and interannual variability of SST in CMIP5 models (e.g., Du & Xie, 2008; Ying et al., 2016). Xie and Philander (1994) linearized the bulk formula to examine the role of surface wind speed changes on the equatorial asymmetry of the intertropical convergence zone. Rahul and Gnanaseelan (2012) examined the mechanisms of LHF trend over the TIO during 1983–2007 based on the linearization method.

They have linked the LHF increase to increase in both SST and surface wind strength. The two dominant modes of interannual climate variability of Indian Ocean such as El Niño Southern Oscillation (ENSO) and Indian Ocean Dipole (IOD) shown to have considerable influence on air-sea flux variability of TIO (Chowdary & Gnanaseelan, 2007). ENSO is characterized by anomalous warming (El Niño) or cooling (La Niña) over the equatorial Pacific Ocean and peaks around December (e.g., Cane & Zebiak, 1985; Philander, 1989). The IOD events are characterized by anomalous cooling in the southeastern equatorial Indian Ocean and anomalous warm SST anomalies in the western

Indian Ocean during its positive phase (PIOD). During the negative phase of IOD (NIOD), enhanced warming of southeastern equatorial Indian Ocean and cooling of western Indian Ocean is observed (Saji et al., 1999; Webster et al., 1999). Q_{net} is a combination of radiative fluxes (shortwave and long wave radiation) and turbulent heat fluxes (latent and sensible flux). So any uncertainties in the estimation of net heat flux are contributed by the uncertainties in each of the components. In situ flux measurements acquired from buoys and ships have long been used as a reference base to quantify the accuracy of surface heat flux products from reanalysis and satellite-based products (e.g., Brunke et al., 2011; Cronin et al., 2006; Josey, 2001; Pinker et al., 2009; Smith et al., 2001; Yu et al., 2004a; Yu et al., 2006). Previous studies have reported significant uncertainty in the estimation of Q_{net} products over the global oceans (e.g., Large & Yeager, 2009; Schott et al., 2009; Yu et al., 2006). These uncertainties are mainly due to the errors in the input parameters (e.g., Large & Yeager, 2009; Rahaman & Ravichandran, 2013) and the bulk algorithms used for estimation of flux component (Brunke et al., 2003; Kalnay et al., 1996; Uppala et al., 2005). The IOD and ENSO frequently coexist with each other (co-occurring events) and they evolve independently (pure events) also. The SST variability evolves in the TIO during ENSO events in response to the cloud-radiation feedback and the wind strength via changes in latent and sensible heat fluxes (Reason et al., 2000). Warming of TIO associated with IOD is mainly caused by the changes in LHF induced by surface wind speed (Yu & Rienecker, 1999). Previous studies on LHF characteristics during ENSO and IOD phases were focused on anomalous basin-wide heating and cooling of the TIO (Chowdary et al., 2006; Chowdary & Gnanaseelan, 2007). However, understanding

distinct signatures of LHF associated with pure and co-occurring events of ENSO and IOD phases is very important as it has several implications on the heat budget of the region.

Accuracy in estimation of the air-sea fluxes over the ocean surface is essential as they represent a medium of communication between the ocean and atmosphere, leading to air-sea interaction processes on diurnal to interdecadal variability. Surface net heat flux (Qnet) plays a crucial role in controlling feedback between the ocean and atmosphere (Yu et al., 2007).

Accurate turbulent flux estimates are essential to assess the energy budget (Dong & Kelly, 2004) as it modulates the mixed layer temperature (Niiler & Kraus, 1977), sea surface temperature (Yu et al., 2006, 2007), heat content (Gartnert & Schott, 1997; Godfrey, 1995), and ocean circulation (Schott et al., 2009). Typically, changes in the Ocean Heat Content of the upper ocean layers can be quantified through the estimation of imbalance of surface flux components.

Thus, accurate surface net heat flux through the heat budget in the upper ocean can give insight into the roles of the atmosphere and ocean in the evolution of sea surface temperature (SST), heat content (Dong & Kelly, 2004), and ocean-atmosphere feedback with changing climate. Therefore, the correct representation of surface fluxes is essential for improving climate models and their forecast skills.

in the estimation of Qnet in various flux products. For example, a recent paper by Valdivieso et al. (2017) reviewed the surface heat fluxes from an ocean reanalysis perspective over the globe using 16 monthly flux products. Bentamy et al. (2017) accessed various turbulent heat flux derived from satellite-based and atmospheric

reanalysis products in spatial and temporal scales and found that all of them exhibit similar space and time patterns with significant differences in magnitude in some specific regions.

More recently, Yu(2019) addresses the dominant source of uncertainties of surface flux products and the reliability of using these products for the budget closures. However, this kind of study of systematic evaluation is lacking over the Indian Ocean. It has been reported in many studies that Indian Ocean SST is crucial for ISMR prediction and is mostly governed by Q_{net} on sea-sonal and intraseasonal time scales (e.g., Parampil et al., 2016; Sengupta & Ravichandran, 2001).

This is important as ocean-atmosphere interactions are critical in maintaining the annual cycle of SST and precipitation (Webster et al., 1998), interannual variability (Saji et al., 1999), and the monsoon intraseasonal oscillations (Sengupta & Ravichandran, 2001). Further, uncertainties of the order of 10 W m^{-2} in Q_{net} estimate may result in uncertainty of $0.5 \text{ }^{\circ}\text{C}$ in SST over three months, implying a strong need for reduction of the uncertainties in Q_{net} to less than 10 W m^{-2} (Roberts, 2011).

Besides, seasonally reversing differences in Q_{net} over the northern and southern tropical IO drive a shallow meridional circulation (Schott & McCreary, 2001) in the tropical IO. While models do simulate the shallow meridional circulation and its variability, it is poorly constrained due to the absence of adequate current observations. For confidence in the simulated shallow meridional circulation by the models, their ability to reproduce Q_{net} correctly is critical. Hence, a comparison of model-simulated Q_{net} with “observation” and reliable estimate of Q_{net} flux products over the IO region is essential. Over the Indian Ocean basin, since the study by Yu et al. (2007) who showed

that the uncertainties in net heatflux could be as significant as 60–100 W/m² over the region, no comprehensive evaluation studies have been carried out over the Indian Ocean afterward.

The southeast Indian Ocean (IO) is a region where extreme climate variability and a unique ocean circulation are observed. During 2010–2011, an extreme marine heat wave associated with ocean warming occurred off the west coast of Australia. This extreme warming event is termed as “Ningaloo Niño” (Feng et al., 2013). The 2010–2011 Ningaloo Niño event was associated with anomalous ocean circulations in the southeast IO. For example, there was an unseasonable surge of the Leeuwin Current, which flows southward against prevailing southerly winds along the west coast of Australia, bringing warm waters from the tropics. These extreme oceanic conditions have a substantial impact on marine ecosystem and regional climate variability (Pearce and Feng, 2013; Wernber et al., 2013; Caputi et al., 2014; Kataoka et al., 2014; Tozuka et al., 2014).

In the southeast IO near the west coast of Australia, relatively large annual mean surface heat fluxes (cooling the ocean) with the strong seasonal cycle are observed (Feng et al., 2003, 2008). For the annual mean, a large amount of heat loss of the ocean occurs at the air-sea interface in a broad area off the west coast of Australia. The majority of the heat loss is caused by a large evaporative cooling due to warm SSTs in the region of the Leeuwin Current. The annual cycle of net surface heat flux is dominated by shortwave radiation and latent heat flux. During the austral winter, shortwave radiation is weak, but the latent heat flux (cooling) is large due to a stronger Leeuwin Current (and thus warm SSTs) and low near-surface specific humidity associated with the cold air temperature. During the austral summer, shortwave radiation is strong, and the latent heat

flux is small due to a weaker Leeuwin Current (Feng et al., 2003, 2008) and higher near-surface specific humidity associated with the warmer air temperature.

In addition to the strong seasonal cycle of air-sea heat fluxes, significant interannual variations of surface heat fluxes are found in this region including those associated with the Ningaloo Niño. Some of the previous studies suggest that the SST warming during the Ningaloo Niño is caused by the heat advection by the strengthening of the Leeuwin Current especially for the 2010–2011 event, whereas air-sea heat fluxes also contribute to the warming (Feng et al., 2013; Zhang et al., 2018). However, the relative importance of heat advection by the Leeuwin Current and surface heat fluxes on the development of the Ningaloo Niño varies substantially between different studies. For example, Benthuisen et al. (2014) indicated that reduced latent and sensible heat fluxes around the peak phase account for 1/3 of the warming during the 2010/2011 event in addition to the heat advection produced by the strengthening of Leeuwin Current.

On the other hand, a composite analysis of multiple Ningaloo Niño events indicated that the initial offshore warming is primarily caused by the anomalous latent heat flux (Marshall et al., 2015). Kataoka et al. (2014) classified the Ningaloo Niño to locally and non-locally amplified modes based on the local wind anomalies and suggested that the reduction of latent heat flux enhances offshore warming during the development and coastal warming during the peak in both modes. Recently, Kataoka et al. (2017) calculated the mixed layer temperature balance associated with Ningaloo Niño events and found that shortwave radiation contributes to the coastal warming in both locally and non-locally amplified modes due to the warming produced by the climatological surface heat flux enhanced by the shallow mixed-layer depth (MLD) anomaly during the onset.

Moreover, Xu et al. (2018) compared the difference in SST warming patterns between the 2012/2013 event with the 2010/2011 event and found that the difference in the relative importance of surface heat fluxes and heat advection between the two events is mostly responsible for the different spatial distribution of the warming.

As described above, a variety of different conclusions on the role of surface heat fluxes in the warming during the Ningaloo Niño have been obtained in previous studies. These differences could partly be due to the different source of surface flux datasets, which include various satellite observations, reanalysis products, and model simulations. The systematic analysis of air-sea heat flux variability associated with the Ningaloo Niño using multiple datasets is thus necessary to reconcile previous studies and determine the uncertainties on the role of air-sea fluxes.

While most of the previous studies focus on processes during the onset and development (warming period) of the Ningaloo Niño, processes that control the cooling during the recovery phase have received little attention. A recent study by Kataoka et al. (2017) discussed processes during both the development and demise of the Ningaloo Niño and suggested that the mixed layer temperature is influenced by not only heat flux anomalies but also MLD anomalies which change the heat capacity. They concluded that the net effect of latent heat flux is not as important as earlier studies suggested

during the recovery phase because of the anomalously deep mixed layers and thus a large heat capacity. In addition, the significant role of sensible heat flux for the locally-amplified mode is suggested.

However, these conclusions are based on the analysis of a single numerical model simulation and it is possible that different results could be obtained using different datasets. Accordingly, it is necessary to examine the processes during the recovery phase using multiple datasets, and such analyses will provide better insights into the role of air-sea fluxes during the recovery phase.

In addition to the large influence of surface heat fluxes on SST and upper ocean during the Ningaloo Niño, air-sea heat fluxes influence the atmospheric conditions and the large-scale atmospheric circulations, and in turn they can feedback on SSTs. Various feedback mechanisms between the atmosphere and ocean associated with the Ningaloo Niño have been suggested in recent years.

For example, Tozuka and Oettli (2018) showed that during the Ningaloo Niño, positive SST anomalies increase the formation of cloud and thus decrease the shortwave radiation, which will weaken the initial warming. Zhang and Han (2018) found that SST anomalies in the southeast IO associated with the Ningaloo Niño lead to the enhancement of western Pacific trade winds and the cooling in the central Pacific.

The enhanced trade winds could strengthen the ITF and the cooling anomalies in the central Pacific could induce cyclonic wind anomalies in the southeast IO, both of which will amplify the initial warming of Ningaloo Niño. As changes in air-sea fluxes in the southeast IO are essential components of these feedback mechanisms, assessing the uncertainties of surface fluxes using multiple datasets is necessary for further exploring these air-sea interaction processes.

The uncertainties of air-sea heat fluxes arise from the errors in bulk atmospheric variables and SST, which are derived from reanalysis products and satellite observations, and use of different bulk flux algorithms (Brunke et al., 2002; Wu et al., 2006; Kubota et al., 2008; Valdivieso et al., 2017). In the area off the west coast of Australia, the uncertainties and thus the difference between the datasets could be very large because of the large variability of SST and associated atmospheric variables caused by Leeuwin Current variations. Hence thorough description of air-sea fluxes in this region using multiple datasets and their comparisons are crucial for the investigation of climate variability in this region including the Ningaloo Niño. The most predominant phenomenon found in the Indian Ocean region is the annual Monsoon reversal.

The physical characteristics of the atmosphere-ocean system demonstrate considerably different characteristics between the summer and winter monsoons. In general, the summer monsoon in the lower atmosphere is dominated by strong west and south westerly flow across south and central India. Strong south easterly trade winds are found in the Southern Hemisphere. Likewise, strong cross-equatorial flow is observed along the east coast of Africa in association with the low-level Somali jet. This cross-equatorial flow is the likely mechanism that transports moisture from the Southern Indian Ocean into the Arabian Sea. (Cadet and Diehl, 1984).

The winter monsoon is characterized by a reversal of this flow. Northeasterlies prevail over the China Sea, Bay of Bengal and Arabian Sea. Although the monsoons are predominately characterized by their overall flow patterns; the intensity of the monsoon is correlated to other surface parameters. Shukla and Misra (1977) found that higher wind speed over the Arabian sea were correlated with lower sea surface temperatures.

The stronger winds lead to increasing evaporation as well as increasing upwelling and subsequent extension of cold coastal waters. The negative correlation between the surface winds and seasurface temperatures was also noted by Cadet and Diehl (1984). Additionally, they determined that weak winds in the Southern Hemisphere and stronger zonal winds along the eastern coast of Africa were associated with a deficit of rainfall over India during the summer. Moreover, warmer sea surface temperature over the Indian Ocean in the summer is responsible for weak atmospheric circulation found during a dry monsoon period. Conversely, colder seasurface temperature was responsible for stronger atmospheric forcing during a wet monsoon. However, this link between sea surface temperature and rainfall is weak according to Weare (1979). More recently, interest in the correlation between the Indian summer monsoon and EN SO has developed. Again, a negative correlation between the Indian Ocean seasurface temperature and the monsoon is indicated. Verma (1992) suggested the warm (cool) phase of ENSO was associated with weaker (stronger) monsoon activity; i.e. less (more) monsoon precipitation.

CHAPTER 3: DATA AND METHODOLOGY

1. Study Area

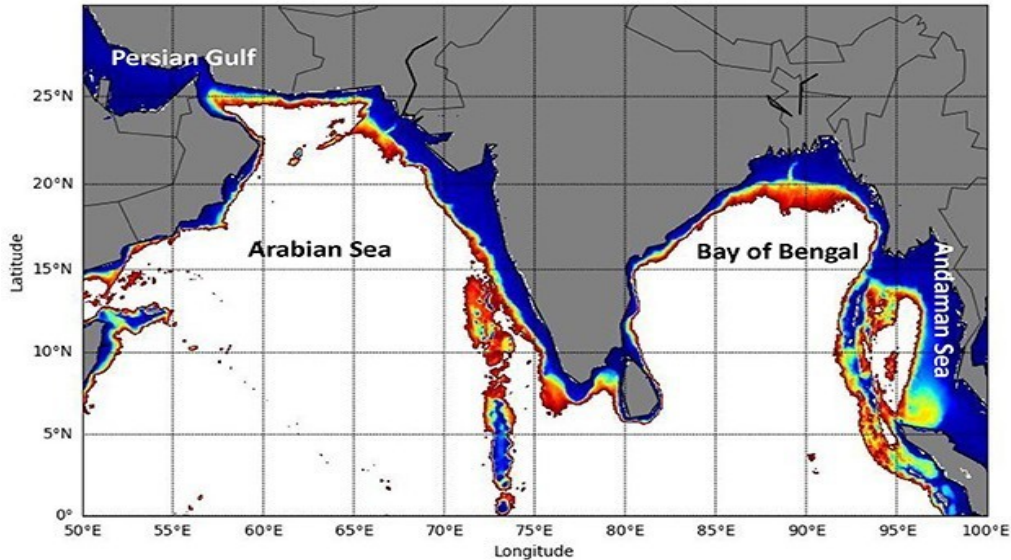


Figure 3.1 Area of Study entire Indian Ocean (–30°N to 30°N Latitude), (40°E to 120°W longitudes)

The area of study is the region from –30°N to 30°N latitudes and 40°E to 120°W longitudes. The Indian Ocean is a vast body of water situated in the Northern Indian Ocean is subdivided by landmasses into the Arabian Sea in the west and the Bay of Bengal in the east and it opens into the equatorial Indian Ocean to the south. The Bay of Bengal coast is shared among India, Bangladesh, Myanmar, Sri Lanka, and the western part of Thailand. The Arabian Sea coast is shared among India, Yemen, Oman, Iran, Pakistan, Sri Lanka, Maldives, and Somalia. The area of interest is the coastal waters of the northern Indian Ocean within the 2,000 m isobath (extending from –30 to 30° N latitude and 40 to 120° E longitude).

2. Data and Sources

a. Sea Surface Temperature (SST)

The data for Sea Surface Temperature (SST) has been downloaded from the CopernicusERA5 <https://cds.climate.copernicus.eu/cdsapp#!/dataset/reanalysis-era5-single-levels?tab=doc> for the duration 2023 with the resolution 0.25x0.25.

b. Sea Level Pressure

Array of 64 bit Reals [TIME = 0..27758]

- **dataset:** http://apdrc.soest.hawaii.edu/dods/public_data/Reanalysis_Data/NCEP/NCEP/daily/surface/lftx4
- **calendar:** GREGORIAN
- **length:** 27759
- **start:** 1948-01-01 00:00:00
- **grads_min:** 00z01jan1948
- **infile_datatype:** DOUBLE
- **units:** days since 0001-01-01 00:00:00
- **point_spacing:** even
- **resolution:** 1.0
- **grads_size:** 27759
- **long_name:** time
- **orig_file_axname:** time
- **grads_mapping:** linear
- **grads_step:** 1dy
- **time_origin:** 0001-01-01 00:00:00
- **maximum:** 00z31dec2023
- **end:** 2023-12-31 00:00:00
- **modulo:** no
- **minimum:** 00z01jan1948
- **grads_dim:** t
- **direction:** L

LAT:- Array of 64 bit Reals [LAT = 0..72]

- **dataset:** http://apdrc.soest.hawaii.edu/dods/public_data/Reanalysis_Data/NCEP/NCEP/daily/surface/lftx4
- **length:** 73
- **start:** -90.0
- **infile_datatype:** DOUBLE

- **units:** degrees_north
 - **point_spacing:** even
 - **resolution:** 2.5
 - **grads_size:** 73
 - **long_name:** latitude
 - **orig_file_axname:** lat
 - **grads_mapping:** linear
 - **maximum:** 90.0
 - **modulo:** no
 - **minimum:** -90.0
 - **grads_dim:** y
 - **direction:** J
- Array of 64 bit Reals [LON = 0..143]
- **dataset:** http://apdrc.soest.hawaii.edu/dods/public_data/Reanalysis_Data/NCEP/NCEP/daily/surface/lftx4
 - **length:** 144
 - **start:** 0.0
 - **infile_datatype:** DOUBLE
 - **units:** degrees_east
 - **point_spacing:** even
 - **resolution:** 2.5
 - **grads_size:** 144
 - **long_name:** longitude
 - **orig_file_axname:** lon
 - **grads_mapping:** linear
 - **maximum:** 357.5
 - **end:** 357.5
 - **modulo:** yes
 - **minimum:** 0.0
 - **grads_dim:** x
 - **direction:** I
- lftx4:Grid
- **direction:** IJL
 - **missing_value:** 1.0E33
 - **_FillValue:** 1.0E33
 - **infile_datatype:** FLOAT
 - **ferret_datatype:** FLOAT
 - **long_name:** best (4-layer) lifted index [degk]
 - **dataset:** http://apdrc.soest.hawaii.edu/dods/public_data/Reanalysis_Data/NCEP/NCEP/daily/surface/lftx4

dataset_index: 1

- Array of 32 bit Reals [TIME = 0..27758][LAT = 0..72][LON = 0..143]
- **direction:** IJL
- **missing_value:** 1.0E33

- **_FillValue:** 1.0E33
 - **infile_datatype:** FLOAT
 - **ferret_datatype:** FLOAT
 - **long_name:** best (4-layer) lifted index [degk]
 - **dataset:** http://apdrc.soest.hawaii.edu/dods/public_data/Reanalysis_Data/NCEP/NCEP/daily/surface/lftx4
 - **dataset_index:** 1
- **TIME:-** Array of 64 bit Reals [TIME = 0..27758]
- **dataset:** http://apdrc.soest.hawaii.edu/dods/public_data/Reanalysis_Data/NCEP/NCEP/daily/surface/lftx4
 - **calendar:** GREGORIAN
 - **length:** 27759
 - **start:** 1948-01-01 00:00:00
 - **grads_min:** 00z01jan1948
 - **infile_datatype:** DOUBLE
 - **units:** days since 0001-01-01 00:00:00
 - **point_spacing:** even
 - **resolution:** 1.0
 - **grads_size:** 27759
 - **long_name:** time
 - **orig_file_axname:** time
 - **grads_mapping:** linear
 - **grads_step:** 1dy
 - **time_origin:** 0001-01-01 00:00:00
 - **maximum:** 00z31dec2023
 - **end:** 2023-12-31 00:00:00
 - **modulo:** no
 - **minimum:** 00z01jan1948
 - **grads_dim:** t
 - **direction:** L
- **LAT:-** Array of 64 bit Reals [LAT = 0..72]
- **dataset:** http://apdrc.soest.hawaii.edu/dods/public_data/Reanalysis_Data/NCEP/NCEP/daily/surface/lftx4
 - **length:** 73
 - **start:** -90.0
 - **infile_datatype:** DOUBLE
 - **units:** degrees_north
 - **point_spacing:** even
 - **resolution:** 2.5
 - **grads_size:** 73
 - **long_name:** latitude
 - **orig_file_axname:** lat
 - **grads_mapping:** linear
 - **maximum:** 90.0
 - **end:** 90.0

- **modulo:** no
 - **minimum:** -90.0
 - **grads_dim:** y
 - **direction:** J

 - **LON:- Array of 64 bit Reals [LON = 0..143]**

 - **dataset:**http://apdrc.soest.hawaii.edu/dods/public_data/Reanalysis_Data/NCEP/NCEP/daily/surface/lftx4

 - **length:** 144
 - **start:** 0.0
 - **infile_datatype:** DOUBLE
 - **units:** degrees_east
 - **point_spacing:** even
 - **resolution:** 2.5
 - **grads_size:** 144
 - **long_name:** longitude
 - **orig_file_axname:** lon
 - **grads_mapping:** linear
 - **maximum:** 357.5
 - **end:** 357.5
 - **modulo:** yes
 - **minimum:** 0.0
 - **grads_dim:** x
- c. Latent Heat Flux:-**

Data Source:- Copernicus

ERA5Product type:

Reanalysis**Variable:** Surface

latent heat flux**Year:** 2023

Month: January, February, March, April, May, June, July, August, September, October, November, December

Day: 01, 02, 03, 04, 05, 06, 07, 08, 09, 10, 11, 12, 13, 14, 15, 16, 17, 18, 19, 20, 21, 22, 23, 24, 25, 26, 27, 28, 29, 30, 31

Time: 00:00, 01:00, 02:00, 03:00, 04:00, 05:00, 06:00, 07:00, 08:00, 09:00, 10:00, 11:00, 12:00, 13:00, 14:00, 15:00, 16:00, 17:00, 18:00, 19:00, 20:00, 21:00, 22:00, 23:00

Sub-region extraction: North 30°, West 20°, South -30°, East 140°

Format:- NetCDF (experimental)

ERA5 hourly data on single levels from 1940 to present

3. METHODOLOGY

The Sea Surface Temperature (SST) data is downloaded from ACopernicus Era5 and is taken from the website on 10 January 2023. The SST concentration data is from January 2023 to December 2023 i.e. for one year and is monthly. The images were obtained showing the region (nIndian Ocean)with variability in the SST distribution using Python Software.

PROGRAM 3.1

The program below plots the area of study bounded Indian Ocean of Figure 3.1 ! 01 January 2023 This program plots long term Sea Surface Temperature (SST), in the Ocean (-30N to 30N, 40E to 120W) on the world map, to study the annual Sea Surface Temperature .

```
import pandas as
pdimport xarray
asxr
import matplotlib.pyplot as plt
from matplotlib.dates import DateFormatter
from matplotlib.ticker import (AutoMinorLocator)
#####
df=xr.open_dataset('/media/linux/Windows-SSD/Goa University/
Copernicus_ERA5_INDIAN_OCEAN_2023_Climatology.nc') #def
kelvinToCelsius(kelvin):return kelvin-273.15
#####
mon=df['time']
sst=df['sst']#-273.15
#####
mon=["Jan", "Feb", "Mar", "Apr", "May", "jun", "Jul", "Aug", "Sep", "Oct", "Nov", "Dec"]
#####
#area_mean_for_yearly=sst_for_yearly.sel(latitude=slice(15,5),
longitude=slice(72,78)).mean(["longitude", "latitude"])
df1=sst.sel(latitude=slice(-30,30), longitude=slice(20,140)).mean(["longitude", "latitude"])
#df2=sst.sel(latitude=slice(12,0), longitude=slice(40,55)).mean(["longitude", "latitude"])
#df3=sst.sel(latitude=slice(25,12), longitude=slice(50,60)).mean(["longitude",
"latitude"])#df4=sst.sel(latitude=slice(18,5), longitude=slice(60,70)).mean(["longitude",
"latitude"])
```



```

#df5=sst.sel(latitude=slice(25,20), longitude=slice(60,70)).mean(["longitude", "latitude"])
#df6=sst.sel(latitude=slice(30,0), longitude=slice(40,78)).mean(["longitude", "latitude"])
#####
fig,ax1=plt.subplots(1,1, figsize=(5,5))
#ax1.xaxis.set_major_formatter(DateFormatter("%m"))
ax1.plot(mon,df1,color='blue',label='South Eastern Box')
#ax1.plot(mon,df2,color='red',label='Somalia South Western Box')
#ax1.plot(mon,df3,color='purple',label='Arabia North Eastern
Box')#ax1.plot(mon,df4,color='green',label='Central Arabian Sea')
#ax1.plot(mon,df5,color='black',label='Northern Box')
#ax1.plot(mon,df6,color='yellow',label='Arabian Sea')
#ax1.plot(df1.time[:,df1.sst[:,color='blue')
#ax1.plot(df4.time[:,df4.sst[:,color='blue')
#ax1.plot(df5.time[:,df5.sst[:,color='blue')
#####
ax1.legend()
ax1.xaxis.set_minor_locator(AutoMinorLocator(4))
#ax1.plot(area_mean_for_5yearly.TIME_COUNTER[2:64],yhat1)#
#ax1.text (10,27.1,'y=0.351x+26.68')
#####
ax1.set_xlabel('Years')ax1.set_ylabel('Temperature (°C)')
fig.suptitle('Seasonal Cycle SST (2023)')
#####
plt.savefig('/media/linux/Windows-SSD/Seasonal Cycle_SST_plot.png')
#####
#file/save

```

PROGRAM 3.2

The program below plots the area of study bounded Indian Ocean of Figure 3.2 ! 01 January 2023 This program plots Climatological Spatial Plot for Sea Surface Temperature (SST), in the Ocean (-30N to 30N, 40E to 120W) on the world map, to study the annual Sea Surface Temperature .

```

#####
import xarray as xr
import matplotlib.pyplot as
pltimport numpy as np

```

```

import cartopy.crs as ccrs
import cartopy.feature as cfeature
#####
#####

nc
=

xr.open_dataset('/media/linux/Windows-SSD/Goa
University/Indian
ocean 2023/
Copernicus_ERA5_INDIAN_OCEAN_2023_Climatology.nc')
#####
#nc_var = nc['slhf']+nc['ssr']+nc['str']
+nc['sshf']nc_var = nc['sst']
#####
nc_var.values=nc_var.values-273.15
#####
# Create a figure with subplots for each month
fig, axes = plt.subplots(3, 4, subplot_kw={'projection': ccrs.PlateCarree()}, figsize=(15,7.5))
#fig.subplots_adjust(left=0.04, right=0.96, bottom=0.05, top=0.95, wspace=-0.59, hspace=0.02)
fig.subplots_adjust(left=0.04, right=0.96, bottom=0.05, top=0.95, wspace=0.1, hspace=-0.1)
#####
#extent = [50, 75, 0, 25]
extent = [20, 140, -30, 30]
#####
# Add map features, e.g., coastlines, to all
subplotsfor ax in axes.flat:
ax.set_extent(extent,
crs=ccrs.PlateCarree())
ax.coastlines(resolution='10m')
# Create a land mask to fill only ocean areas with
contoursland_mask
=
cfeature.NaturalEarthFeature('physical',
'land',
'10m',
edgecolor='face',

```

```

facecolor='none')
#####
mons=['Jan','Feb','Mar','Apr','May','Jun','Jul','Aug','Sep','Oct','Nov','Dec']
#slno=['(jan)','(b)','(c)','(d)','(e)','(f)','(g)','(h)','(i)','(j)','(k)','(l)']
#####
# Loop through each month and plot the
climatologyfor i, ax in enumerate(axes.flat):
month_number = i + 1 # Months are 1-based
contour = nc_var.isel(time=month_number - 1).plot.contourf(ax=ax, levels=np.arange(20, 35, 1),
cmap='jet', add_colorbar=False)
ax.add_feature(land_mask, zorder=1, edgecolor='none', facecolor='grey')
ax.set_title(mons[i],zorder=2,fontsize=12,fontweight='bold',family='serif',color='black',y=
0.05,
x=0.75)#####
# Add a background or bounding box behind the subplot label
#ax.annotate(slno[i], xy=(0.05, 0.85), xycoords='axes fraction', fontsize=12,
fontweight='bold',# bbox=dict(boxstyle='square', pad=0.3', edgecolor='black',
facecolor='White'),
# textcoords='axes fraction',family='serif')
#####
if (i==0 or i==4 or i==8): # Y Axis to first column
ax.set_yticks(np.arange(-30, 30, 30), crs=ccrs.PlateCarree())
ax.set_yticks(np.arange(-30, 30, 1), minor=True,
crs=ccrs.PlateCarree())ax.yaxis.set_tick_params(width=1,
which='major',direction='in') ax.yaxis.set_tick_params(width=0.5,
which='minor',direction='in') #ax.set_yticklabels([f'{tick}°N' for tick
inax.get_yticks()])
for label in ax.get_yticklabels():
label.set_fontsize(12)
label.set_fontweight('bold')
label.set_family('serif')
label.set_rotation(90)
label.set_verticalalignment('center')
ax.set_ylabel("")
#####
if (i==8 or i==9 or i==10 or i==11): # X Axis to last row
ax.set_xticks(np.arange(20, 140, 50), crs=ccrs.PlateCarree())
ax.set_xticks(np.arange(20, 140, 1), minor=True, crs=ccrs.PlateCarree())

```

```

ax.xaxis.set_tick_params(width=1, which='major',direction='in')
ax.xaxis.set_tick_params(width=0.5,
which='minor',direction='in')ax.set_xticklabels([f '{tick}°E' for
tick in ax.get_xticks()])
for label in ax.get_xticklabels():
label.set_fontsize(12)
label.set_fontweight('bold')
label.set_family('serif')
ax.set_xlabel("")
fig.suptitle('Indian Ocean', fontsize=30)
#####
colorbar_ticks = [20,25,30, 35]
cbar = plt.colorbar(contour, ax=axes.ravel().tolist(), orientation='horizontal', pad=0.05, aspect=30,
shrink=0.7, ticks=colorbar_ticks, extend='both',extendfrac=0)
cbar.set_label("SST (°C)", fontsize=12,
fontweight='bold',family='serif')tick_labels = cbar.ax.get_xticklabels()
for label in tick_labels:
label.set_fontweight('bold')
label.set_fontsize(12)
label.set_family('serif')
#####
#plt.tight_layout()
plt.show()
#####

```

PROGRAM 3.3

The program below plots the area of study bounded Indian Ocean of Figure 3.3 ! 01 nd January 2023 This program plots Climatological Spatial Plot for Latent Heat Flux (SST), in the Ocean (- 30N to 30N, 40E to 120W) on the world map, to study the Climatological Latent Heat Flux.

```

# Necessary
Librariesimport
xarray as xr
import matplotlib.pyplot as plt
import numpy as np
import cartopy.crs as ccrs

```

```

import cartopy.feature as cfeature
from cartopy.mpl.gridliner import LONGITUDE_FORMATTER, LATITUDE_FORMATTER
import calendar
#import matplotlib.ticker as
mticker# Open the NetCDF file
dataset = xr.open_dataset('/media/linux/Windows-SSD/Goa University/
Copernicus_ERA5_SURFACE_Latent_INDIAN_OCEAN_Climatology_2023.nc') sst=dataset['slhf']#/
1000
clevels=np.arange(100.0,104.0,0.5)
#sst=dataset['tp']
#sst=('e-tp')
# Replace 'variable_name' with the name of the variable you want to plot
#variable_name = 'time_bnds'
sst1=sst.sel(latitude=slice(30,-30), longitude=slice(20,120))
#xx=sst1.sel(latitude=10,longitude=65).isel(time=4)# Create a figure with subplots for each
monthfig, ax = plt.subplots(3, 4, subplot_kw={'projection': ccrs.PlateCarree()}, figsize=(15, 10))
fig.subplots_adjust(left=0.04, right=0.96, bottom=0.05, top=0.95, wspace=0.2, hspace=0.1)
#fig,ax = width = cell_width * ncols + 2
# Create a land mask to fill only ocean areas with contours
pl=ax[0,0].contourf(sst1.longitude, sst1.latitude,sst1[0,:,:], cmap='jet',
extend='both')ax[0,1].contourf(sst1.longitude, sst1.latitude,sst1[1,:,:],
cmap='jet',extend='both') ax[0,2].contourf(sst1.longitude, sst1.latitude,sst1[2,:,:],
cmap='jet',extend='both') ax[0,3].contourf(sst1.longitude, sst1.latitude,sst1[3,:,:],
cmap='jet',extend='both') ax[1,0].contourf(sst1.longitude, sst1.latitude,sst1[4,:,:],
cmap='jet',extend='both') ax[1,1].contourf(sst1.longitude, sst1.latitude,sst1[5,:,:],
cmap='jet',extend='both') ax[1,2].contourf(sst1.longitude, sst1.latitude,sst1[6,:,:],
cmap='jet',extend='both') ax[1,3].contourf(sst1.longitude, sst1.latitude,sst1[7,:,:],
cmap='jet',extend='both') ax[2,0].contourf(sst1.longitude, sst1.latitude,sst1[8,:,:],
cmap='jet',extend='both') ax[2,1].contourf(sst1.longitude, sst1.latitude,sst1[9,:,:],
cmap='jet',extend='both') ax[2,2].contourf(sst1.longitude, sst1.latitude,sst1[10,:,:],
cmap='jet',extend='both') ax[2,3].contourf(sst1.longitude, sst1.latitude,sst1[11,:,:],
cmap='jet',extend='both') #pl=ax.ylabel('Evaporation (m/day)')
#ax[2,0].add_feature(cfeatures.LAND, zorder=10, color='navajowhite',
alpha=0.1)#ax[2,0].add_feature(cfeature.LAND,color='grey')
ax[0,0].add_feature(cfeature.COASTLINE,zorder=10,lw=2,color='black')

```

```

ax[0,1].add_feature(cfeature.COASTLINE,zorder=10,lw=2,color='black')
ax[0,2].add_feature(cfeature.COASTLINE,zorder=10,lw=2,color='black')
ax[0,3].add_feature(cfeature.COASTLINE,zorder=10,lw=2,color='black')
ax[1,0].add_feature(cfeature.COASTLINE,zorder=10,lw=2,color='black')
ax[1,1].add_feature(cfeature.COASTLINE,zorder=10,lw=2,color='black')
ax[1,2].add_feature(cfeature.COASTLINE,zorder=10,lw=2,color='black')
ax[1,3].add_feature(cfeature.COASTLINE,zorder=10,lw=2,color='black')
ax[2,0].add_feature(cfeature.COASTLINE,zorder=10,lw=2,color='black')
ax[2,1].add_feature(cfeature.COASTLINE,zorder=10,lw=2,color='black')
ax[2,2].add_feature(cfeature.COASTLINE,zorder=10,lw=2,color='black')
ax[2,3].add_feature(cfeature.COASTLINE,zorder=10,lw=2,color='black')
#####
ax[0,0].add_feature(cfeature.LAND,zorder=10,color='white')
ax[0,1].add_feature(cfeature.LAND,zorder=10,color='white')
ax[0,2].add_feature(cfeature.LAND,zorder=10,color='white')
ax[0,3].add_feature(cfeature.LAND,zorder=10,color='white')
ax[1,0].add_feature(cfeature.LAND,zorder=10,color='white')
ax[1,1].add_feature(cfeature.LAND,zorder=10,color='white')
ax[1,2].add_feature(cfeature.LAND,zorder=10,color='white')
ax[1,3].add_feature(cfeature.LAND,zorder=10,color='white')
ax[2,0].add_feature(cfeature.LAND,zorder=10,color='white')
ax[2,1].add_feature(cfeature.LAND,zorder=10,color='white')
ax[2,2].add_feature(cfeature.LAND,zorder=10,color='white')
ax[2,3].add_feature(cfeature.LAND,zorder=10,color='white')
#height = cell_height * nrows + 2 * margin
ax[0,0].set_yticks(np.arange(-30,30,10.))
#ax[0,0].set_xticks(np.arange(20,120,10.))
#ax[0,1].set_yticks(np.arange(-30,30,10.))
#ax[0,1].set_xticks(np.arange(20,120,10.))
#ax[0,2].set_yticks(np.arange(-30,30,10.))
#ax[0,2].set_xticks(np.arange(40,78,5.))#ax[0,3].set_yticks(np.arange(0,30,5.))
#ax[0,3].set_xticks(np.arange(40,78,5.))
ax[1,0].set_yticks(np.arange(-30,30,10.))
)#ax[1,0].set_xticks(np.arange(40,78,5.))
#ax[1,1].set_yticks(np.arange(0,30,5.))

```

```

#ax[1,1].set_xticks(np.arange(40,78,5.))
#ax[1,2].set_yticks(np.arange(0,30,5.))
#ax[1,2].set_xticks(np.arange(40,78,5.))
#ax[1,3].set_yticks(np.arange(0,30,5.))
#ax[1,3].set_xticks(np.arange(20,120,10.))
ax[2,0].set_yticks(np.arange(-30,30,10.))
ax[2,0].set_xticks(np.arange(20,120,10.))
#ax[2,1].set_yticks(np.arange(0,30,5.))
ax[2,1].set_xticks(np.arange(20,120,10.))
#ax[2,2].set_yticks(np.arange(0,30,5.))
ax[2,2].set_xticks(np.arange(20,120,10.))
ax[2,3].set_yticks(np.arange(-30,30,10.))
ax[2,3].set_xticks(np.arange(20,120,10.))
#ax.set_ylabel('Temperature (°C)')
ax[0,0].set_title('Jan', fontsize=20)
ax[0,1].set_title('Feb', fontsize=20)
ax[0,2].set_title('Mar', fontsize=20)
ax[0,3].set_title('Apr', fontsize=20)
ax[1,0].set_title('May', fontsize=20)
ax[1,1].set_title('June', fontsize=20)
ax[1,2].set_title('July', fontsize=20)
ax[1,3].set_title('Aug', fontsize=20)
ax[2,0].set_title('Sep', fontsize=20)
ax[2,1].set_title('Oct', fontsize=20)
ax[2,2].set_title('Nov', fontsize=20)
ax[2,3].set_title('Dec', fontsize=20)
#ax[0,0].text(62,13,'Jan')
#ax[0,1].text(62,13,'Feb')
fig.suptitle('INDIANOCEAN ', fontsize=30)
cbar=plt.colorbar(pl,ax=ax)
cbar.set_label(' Latent Heat Flux (W/m2)',
fontsize=20)#ax.ylabel('Evaporation (m/day)')
plt.savefig('/media/linux/Windows-SSD/Evaporation_Spatial_data.jpg')
#plt.show()'''

```

PROGRAM 3.4

The program below plots the area of study bounded Indian Ocean of Figure 3.4 ! 01 January 2023
This program plots Climatological Spatial Plot for Sea Level Pressure , in the Ocean (-30N to 30N,
40E to 120W) on the world map, to study the Climatological Sea level pressure.

```
import xarray as xr
import matplotlib.pyplot as plt
import numpy as np
import cartopy.crs as ccrs
import cartopy.feature as cfeature
from cartopy.mpl.gridliner import LONGITUDE_FORMATTER, LATITUDE_FORMATTER
import calendar
#import matplotlib.ticker as mticker

# Open the NetCDF file
dataset = xr.open_dataset('/media/linux/Windows-SSD/Goa
University/Latent_Heat_Flux_Climatology_IndianOcean_2023.nc')
sst=dataset['SLP']/1000
clevels=np.arange(100.0,104.0,0.5)
#sst=dataset['tp']
#sst=('e-tp')
# Replace 'variable_name' with the name of the variable you want to plot
#variable_name = 'time_bnds'
sst1=sst.sel(LAT7_49=slice(-30,30), LON9_49=slice(20,120))

#xx=sst1.sel(latitude=10,longitude=65).isel(time=4)

# Create a figure with subplots for each month
fig, ax = plt.subplots(3, 4, subplot_kw={'projection': ccrs.PlateCarree()}, figsize=(15, 10))
fig.subplots_adjust(left=0.04, right=0.96, bottom=0.05, top=0.95, wspace=0.2, hspace=0.1)
#fig,ax = width = cell_width * ncols + 2
# Create a land mask to fill only ocean areas with contours
pl=ax[0,0].contourf(sst1.LON9_49, sst1.LAT7_49,sst1[0,:,:],
cmap='jet',levels=clevels)ax[0,1].contourf(sst1.LON9_49, sst1.LAT7_49,sst1[1,:,:],
cmap='jet',levels=clevels) ax[0,2].contourf(sst1.LON9_49, sst1.LAT7_49,sst1[2,:,:],
cmap='jet',levels=clevels) ax[0,3].contourf(sst1.LON9_49, sst1.LAT7_49,sst1[3,:,:],
cmap='jet',levels=clevels) ax[1,0].contourf(sst1.LON9_49, sst1.LAT7_49,sst1[4,:,:],
cmap='jet',levels=clevels) ax[1,1].contourf(sst1.LON9_49, sst1.LAT7_49,sst1[5,:,:],
cmap='jet',levels=clevels) ax[1,2].contourf(sst1.LON9_49, sst1.LAT7_49,sst1[6,:,:],
cmap='jet',levels=clevels) ax[1,3].contourf(sst1.LON9_49, sst1.LAT7_49,sst1[7,:,:],
cmap='jet',levels=clevels) ax[2,0].contourf(sst1.LON9_49, sst1.LAT7_49,sst1[8,:,:],
cmap='jet',levels=clevels) ax[2,1].contourf(sst1.LON9_49, sst1.LAT7_49,sst1[9,:,:],
cmap='jet',levels=clevels) ax[2,2].contourf(sst1.LON9_49, sst1.LAT7_49,sst1[10,:,:],
cmap='jet',levels=clevels) ax[2,3].contourf(sst1.LON9_49, sst1.LAT7_49,sst1[11,:,:],
cmap='jet',levels=clevels) #pl=ax.ylabel('Evaporation (m/day)')
#ax[2,0].add_feature(cfeatures.LAND, zorder=10, color='navajowhite', alpha=0.1)
#ax[2,0].add_feature(cfeature.LAND,color='grey')
ax[0,0].add_feature(cfeature.COASTLINE,zorder=10,lw=2,color='black')
```

```

ax[0,1].add_feature(cfeature.COASTLINE,zorder=10,lw=2,color='black')
ax[0,2].add_feature(cfeature.COASTLINE,zorder=10,lw=2,color='black')
ax[0,3].add_feature(cfeature.COASTLINE,zorder=10,lw=2,color='black')
ax[1,0].add_feature(cfeature.COASTLINE,zorder=10,lw=2,color='black')
ax[1,1].add_feature(cfeature.COASTLINE,zorder=10,lw=2,color='black')
ax[1,2].add_feature(cfeature.COASTLINE,zorder=10,lw=2,color='black')
ax[1,3].add_feature(cfeature.COASTLINE,zorder=10,lw=2,color='black')
ax[2,0].add_feature(cfeature.COASTLINE,zorder=10,lw=2,color='black')
ax[2,1].add_feature(cfeature.COASTLINE,zorder=10,lw=2,color='black')
ax[2,2].add_feature(cfeature.COASTLINE,zorder=10,lw=2,color='black')
ax[2,3].add_feature(cfeature.COASTLINE,zorder=10,lw=2,color='black')
#####
ax[0,0].add_feature(cfeature.LAND,zorder=10,color='white')
ax[0,1].add_feature(cfeature.LAND,zorder=10,color='white')
ax[0,2].add_feature(cfeature.LAND,zorder=10,color='white')
ax[0,3].add_feature(cfeature.LAND,zorder=10,color='white')
ax[1,0].add_feature(cfeature.LAND,zorder=10,color='white')
ax[1,1].add_feature(cfeature.LAND,zorder=10,color='white')
ax[1,2].add_feature(cfeature.LAND,zorder=10,color='white')
ax[1,3].add_feature(cfeature.LAND,zorder=10,color='white')
ax[2,0].add_feature(cfeature.LAND,zorder=10,color='white')
ax[2,1].add_feature(cfeature.LAND,zorder=10,color='white')
ax[2,2].add_feature(cfeature.LAND,zorder=10,color='white')
ax[2,3].add_feature(cfeature.LAND,zorder=10,color='white')
#height = cell_height * nrows + 2 * margin
ax[0,0].set_yticks(np.arange(-30,30,10.))
#ax[0,0].set_xticks(np.arange(20,120,10.))
#ax[0,1].set_yticks(np.arange(-30,30,10.))
#ax[0,1].set_xticks(np.arange(20,120,10.))
#ax[0,2].set_yticks(np.arange(-30,30,10.))
#ax[0,2].set_xticks(np.arange(40,78,5.))
#ax[0,3].set_yticks(np.arange(0,30,5.))
#ax[0,3].set_xticks(np.arange(40,78,5.))
ax[1,0].set_yticks(np.arange(-30,30,10.))
#ax[1,0].set_xticks(np.arange(40,78,5.))
#ax[1,1].set_yticks(np.arange(0,30,5.))
#ax[1,1].set_xticks(np.arange(40,78,5.))
#ax[1,2].set_yticks(np.arange(0,30,5.))
#ax[1,2].set_xticks(np.arange(40,78,5.))
#ax[1,3].set_yticks(np.arange(0,30,5.))
#ax[1,3].set_xticks(np.arange(20,120,10.))
ax[2,0].set_yticks(np.arange(-30,30,10.))
ax[2,0].set_xticks(np.arange(20,120,10.))
#ax[2,1].set_yticks(np.arange(0,30,5.))
ax[2,1].set_xticks(np.arange(20,120,10.))
#ax[2,2].set_yticks(np.arange(0,30,5.))
ax[2,2].set_xticks(np.arange(20,120,10.))
ax[2,3].set_yticks(np.arange(-30,30,10.))
ax[2,3].set_xticks(np.arange(20,120,10.))
#ax.set_ylabel('Temperature (°C)')
ax[0,0].set_title('Jan', fontsize=20)
ax[0,1].set_title('Feb', fontsize=20)

```

```

ax[0,2].set_title('Mar', fontsize=20)
ax[0,3].set_title('Apr', fontsize=20)
ax[1,0].set_title('May', fontsize=20)
ax[1,1].set_title('June', fontsize=20)
ax[1,2].set_title('July', fontsize=20)
ax[1,3].set_title('Aug', fontsize=20)
ax[2,0].set_title('Sep', fontsize=20)
ax[2,1].set_title('Oct', fontsize=20)
ax[2,2].set_title('Nov', fontsize=20)
ax[2,3].set_title('Dec', fontsize=20)
#ax[0,0].text(62,13,'Jan')
#ax[0,1].text(62,13,'Feb')
fig.suptitle('INDIANOCEAN ', fontsize=30)

cbar=plt.colorbar(pl,ax=ax)
cbar.set_label('Temp (°C)',
fontsize=20)#ax.ylabel('Evaporation (m/
day)')

plt.savefig('/media/linux/Windows-SSD/Evaporation_Spatial_data.jpg')
#plt.show()

```

CHAPTER 4: OBSERVATIONS

1. MAPS OF Sea Surface Temperature (SST) -A CONCENTRATION AVERAGED FROM JANUARY TO DECEMBER 2023 (Time Series)

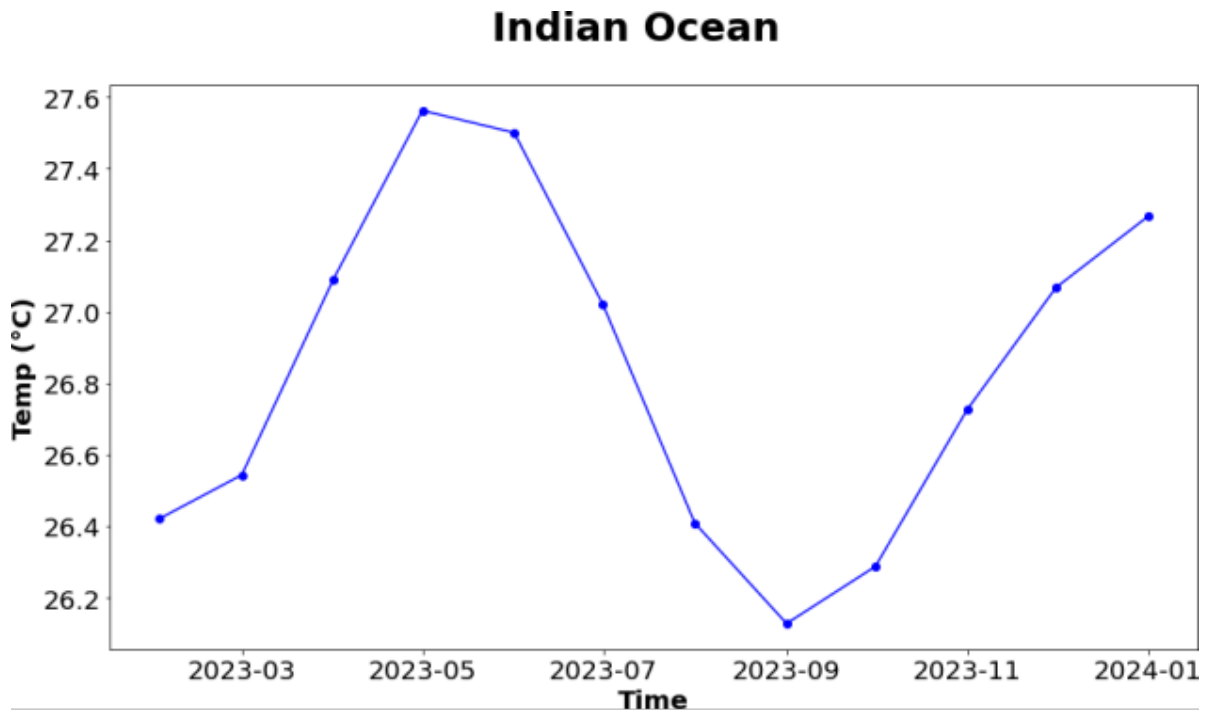


Figure 4.1 – Sea Surface Temperature (SST) concentration map (Degree Celcius) in the Indian Ocean (-30 °N to 30 °N, 40 °E to 120 °W), averaged in the period from January 2023 to December 2023.

In the Indian Ocean (Latitude 20-140), Longitude (-30-30) shows the Sea Surface Temperature (SST) ranges between 26.2 °C-27.6°C. The lowest temperature was in the month of August to September (26.2°C) and the highest sea surface temperature (SST) in the Indian Ocean was observed between the month of April to May (27.5 °C) respectively in the month of June. The Sea Surface temperature in the Indian Ocean was observed with the increasing trend from February respectively in September. However, the SST in the decreasing trend was observed

between June to September. Overall the major fluctuations of Sea Surface Temperature in the Indian Ocean was observed from February respectively May and September.

2. MAPS OF Sea Surface Temperature (SST) -A CONCENTRATION AVERAGED FROM JANUARY TO DECEMBER 2023 (Climatological)

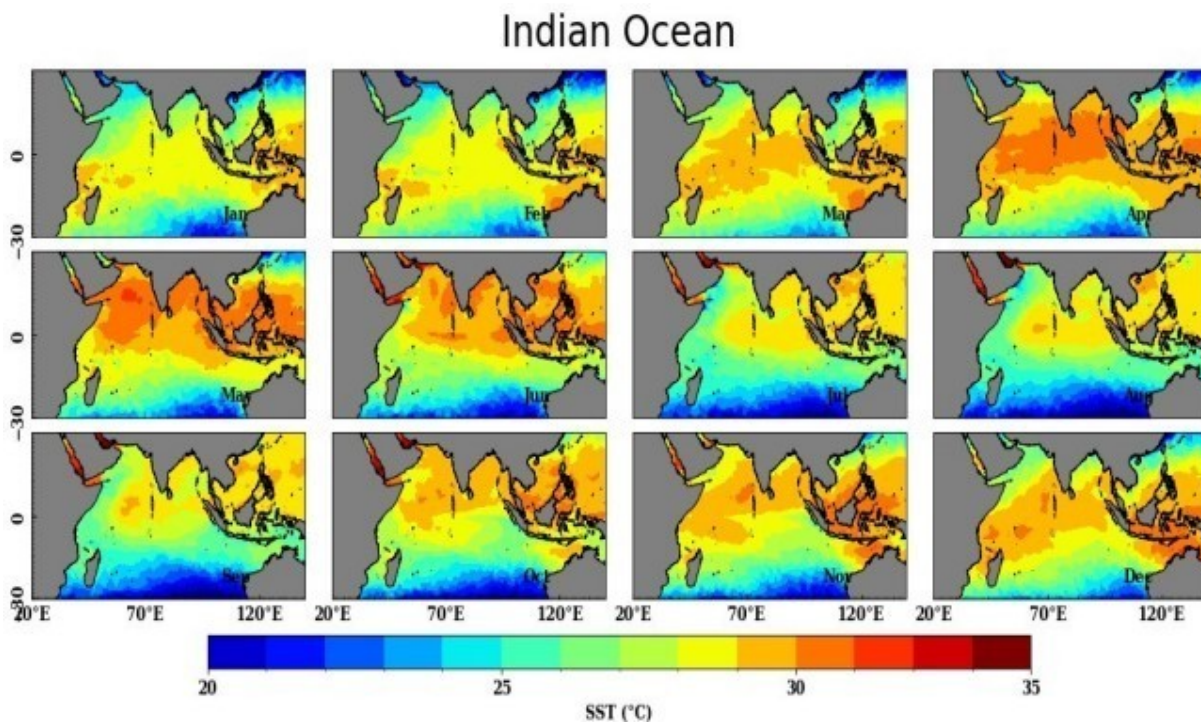


Figure 4.2 – Sea Surface Temperature (SST) concentration map (Degree Celcius) in the Indian Ocean (-30 °N to 30 °N, 40 °E to 120 °W), averaged in the period from January 2023 to December 2023. (Climatological)

In the entire Indian Ocean (Latitude 20-140), Longitude (-30-30) Spatial plots SEa Surface Temperature (Climatology) shows almost warmer in the central Indian Ocean and the Sea Surface Temperature (SST) ranges between 21 °C to ≈30 °C. The lowest temperature was in the month of January respectively in February and August (≈26.2°C) and the highest sea surface temperature (SST) in the Indian Ocean was observed between the month of April to May (≈27.5 °C) respectively in the month of June. Moreover, mainly April, May and June showed the

highest sea surface temperature in the Indian Ocean compare to the other months. However, January and February showed almost similar to each other. May and June showed highest SST towards South West Coast of India. Similarly from July onward the SST shown in decreasing trend . Compare to May and June SST slightly decreased in the month July and August and remained decreasing till February October and November shown almost similar.

3. MAPS OF Latent Heat Flux (LHF) -A CONCENTRATION AVERAGED FROM JANUARY TO DECEMBER 2023 (Climatological)

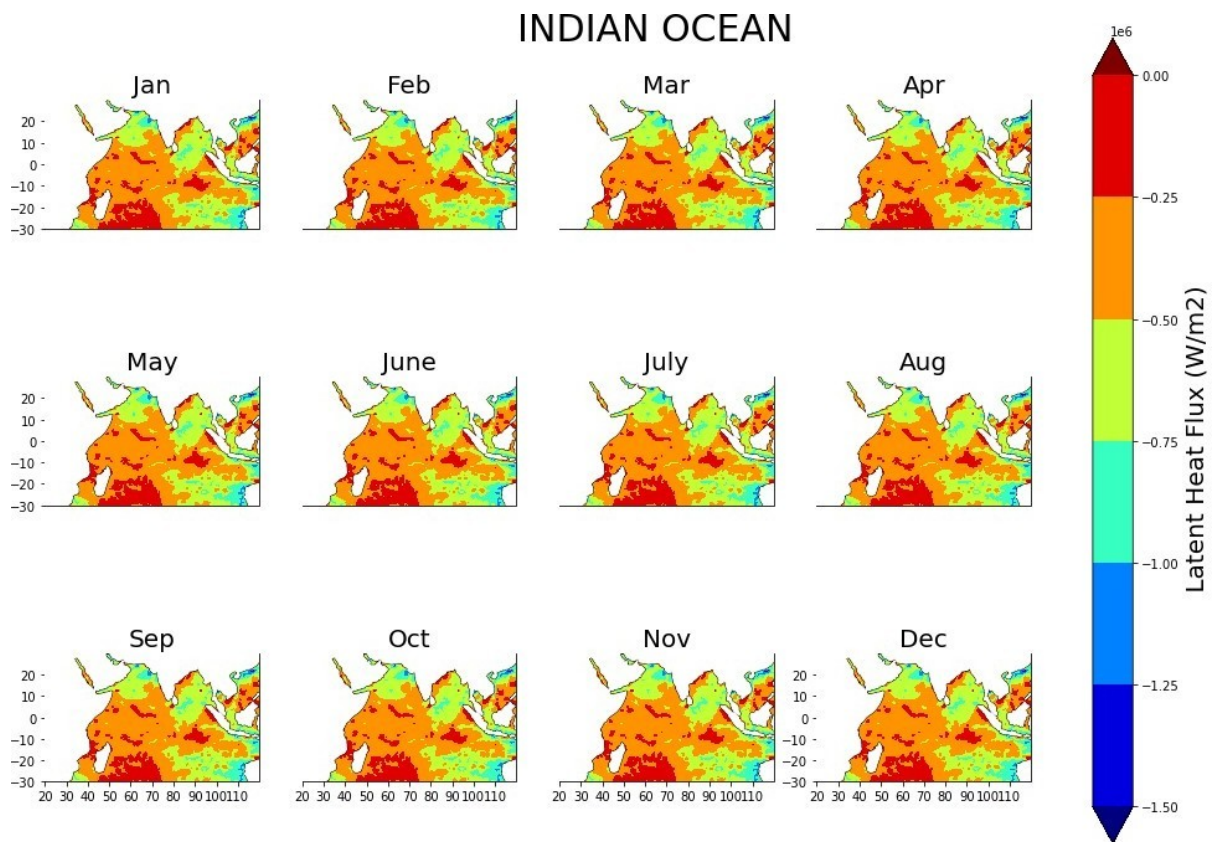


Figure 4.3 – Latent Heat Flux (LHF) concentration map (w/m2) in the Indian Ocean (-30 °N to 30 °N, 40 °E to 120 °W), averaged in the period from January 2023 to December 2023. (Climatological)

The map of the Latent Heat Flux concentration averaged in the months of January, in the period from July 20023 to December 2023, is shown in the Figure 4.3 The Latent Heat Flux concentration map shows a minimum value of -1.50 w/m^2 and a maximum value of 0.00 w/m^2 . -0.75 to -0.50 Higher values of Heat Flux concentration are seen closer to the coastal regions in general. Values above -0.25 w/m^2 are seen along many parts of the central Indian Ocean, especially closer to the Arabian Sea and also between the -20°N and 70°N latitudes . There are also smaller regions along the coast parts of the Indian Ocean 0°N and 110°N latitudes region where the latent heat flux occurred between -0.75 to -0.50 w/m^2 .

4. MAPS OF Sea Level Pressure (SLP) -A CONCENTRATION AVERAGED FROM JANUARY TO DECEMBER 2023 (Climatological)

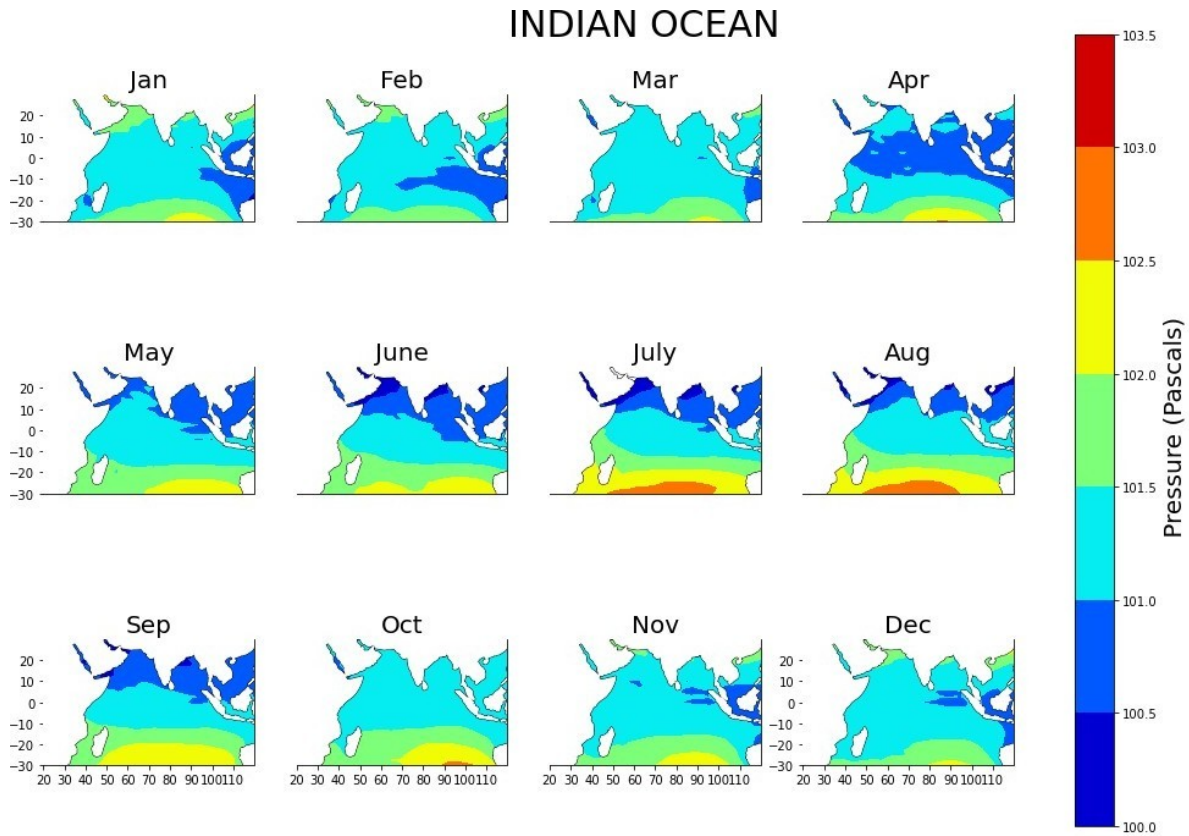


Figure 4.4 – Sea Level Pressure (SLP) concentration map (pascals) in the Indian Ocean (-30 °N to 30 °N, 40 °E to 120 °W), averaged in the period from January 2023 to December 2023.

(Climatological)

The partial pressure in the Indian Ocean (latitude -30 and 30 °E and longitude 40 °E to 120 °W) ranges between 100 to 103 pascals. The highest pressure in July and August was observed and the lowest was in April. Similarly in the month of May, June and July the partial pressure was almost similar that ranges between 100-101 pascal. During October and November pressure ranges between 101 to 101.5 pascal.

The map of Sea Level Pressure concentration averaged in the months of January, October, November and December in the period from July 2003 to April 2023 is shown in the Figure 4.4. The Sea Level Pressure concentration map shows a minimum value of 100.0 (Pascal) and a maximum value of 103.5 (pascals). Higher values of pressure concentration observed to the coast (latitude -20 and 10 °E and longitude 60 °E to 90 °W) in the month of July and August. Values above 102 pascals observed along many parts of the coast of Indian Ocean.

CHAPTER 5: DISCUSSION

The values of the basin-averaged Sea Surface Temperature (SST) concentration, Latent Heat Flux, Oceanic Pressure slopes of trend- lines, and climatological studies in the Indian Ocean (-30°N to 30°N, 40°E to 120°W), are shown averaged for entire time-period, month wise, season wise, in the period from January 2003 to December 2023, in Table 5.1. Table 5.1 – Values of the entire Indian Ocean (-30°N to 30°N, 40°E to 120°W) basin-averaged pressure but the concentration of Sea Surface Temperature completely vary from one to another parts of the Indian Ocean time-series, month-wise and season-wise, in the period from January 2003 to December 2023.

Entire Time-period / Averaged Slopes Sea Surface Temperature	Averaged Sea Surface Temperature (Degree Celcius)	Averaged Sea Level Pressure (Pascals)	Averaged Latent Heat Flux (w/m ²)
January	26.3	101.0-101.5	-0.75
February	26.4	101.0	-0.50
March	26.4	101.0-101.5	-0.75
April	25.2	100.5	--0.75
May	27.6	101.2	-0.75
June	27.5	100.5	-0.75
July	27.2	101.0	-0.75
August	26.3	101.0-101.5	-0.75
September	26.4	100.5	-0.75

October	26.6	101.0	-0.75
November	27.2	101.5	-0.75
December	27.3	101.0	-0.75

Table .5.1. Table shows different variables of parameters sea surface temperature SST, Pressure, Latent Heat Flux

CHAPTER 6: CONCLUSIONS

Time Series Sea Surface Temperature varies from January to December in the entire Indian Ocean, the highest temperature peak was observed in the month of May respectively June that ranges between 26-27.2 degree Celsius. Similarly the lowest rate of Sea Surface Temperature was observed in the month between November to January due to winter. The highest variation in the temperature observed after March. Overall the pressure in the Indian Ocean remained almost similar in every month but the temperature completely differed from month to month. Overall latent Heat Flux indirectly correlated with Temperature in the Indian Ocean. Specially in the Central Indian Ocean the variation was slightly similar compare to coastal zone.

Latent Heat Flux showed almost similar in the Indian Ocean monthly but there must be possibility to study long term warming and latent Heat Flux along with different Parameter in the Indian Ocean to obtain high impact of Short wave and long wave radiation and physical factors in the Indian Ocean.

REFERENCE LIST

1. Zhao, N., G. Zhang, S. Zhang, Y. Bai, S. Ali, and J. Zhang. 2019. Temporal-Spatial Distribution of Chlorophyll-a and Impacts of Environmental Factors in the Bohai Sea and Yellow Sea. *IEEEAccess: Open Access Journal*, 7, 160947–160960. d.o.i.: 10.1109/ACCESS.2019.2950833
2. Zhang, W-Z., H. Wang, F. Chai, and G. Qiu. 2016. Physical Drivers of Chlorophyll Variability in the Open South China Sea. *Journal of Geophysical Research: Oceans*, 121, 7123– 7140. d.o.i.:<https://doi.org/10.1002/2016JC011983>
3. Yu, Lisan, Xiangze Jin, and Robert A. Weller. "Annual, seasonal, and interannual variability of air–sea heat fluxes in the Indian Ocean." *Journal of climate* 20, no. 13 (2007): 3190-3209.
4. Yu, Lisan, Xiangze Jin, and Robert A. Weller. "Annual, seasonal, and interannual variability of air–sea heat fluxes in the Indian Ocean." *Journal of climate* 20, no. 13 (2007): 3190-3209.
5. Raj Parampil, Sindu, G. N. Bharathraj, Matthew Harrison, and Debasis Sengupta. "Observed subseasonal variability of heat flux and the SST response of the tropical
6. Indian Ocean." *Journal of Geophysical Research: Oceans* 121, no. 10 (2016): 7290-7307.
7. McPhaden, M. J., Busalacchi, A. J., Cheney, R., Donguy, J. R., Gage, K. S., Halpern, D., ...& Takeuchi, K. (1998). The Tropical Ocean-Global Atmosphere observing system: A decade of progress. *Journal of Geophysical Research: Oceans*, 103(C7), 14169-14240.
8. 1. Lee, S. K., Park, W., Baringer, M. O., Gordon, A. L., Huber, B., & Liu, Y. (2015). Pacific origin of the abrupt increase in Indian Ocean heat content during the warming hiatus. *Naturegeoscience*, 8(6), 445-449.
9. 2. Lee SK, Park W, Baringer MO, Gordon AL, Huber B, Liu Y. Pacific origin of the abrupt increase in Indian Ocean heat content during the warming hiatus. *Nature geoscience*. 2015 Jun;8(6):445-9.
10. Ummenhofer, Caroline C., Sujata A. Murty, Janet Sprintall, Tong Lee, and Nerilie J. Abram. "Heat and freshwater changes in the Indian Ocean region." *Nature Reviews Earth & Environment* 2,no. 8 (2021): 525-541.

11. Vranes, Kevin, Arnold L. Gordon, and Amy Field. "The heat transport of the Indonesian Throughflow and implications for the Indian Ocean heat budget." *Deep Sea Research Part II: Topical Studies in Oceanography* 49, no. 7-8 (2002): 1391-1410.
12. Zhang, Lei, Weiqing Han, Yuanlong Li, and Nicole S. Lovenduski. "Variability of sea level and upper-ocean heat content in the Indian Ocean: Effects of subtropical Indian Ocean dipole and ENSO." *Journal of Climate* 32, no. 21 (2019): 7227-7245.
13. Ma, Jie, Ming Feng, Jian Lan, and Dunxin Hu. "Projected future changes of meridional heat transport and heat balance of the Indian Ocean." *Geophysical Research Letters* 47, no. 4 (2020): e2019GL086803.
14. through the floor of the Indian Ocean." *Journal of Geophysical Research* 82.23 (1977): 3391-3409.
15. Volkov DL, Lee SK, Gordon AL, Rudko M. Unprecedented reduction and quick recovery of the South Indian Ocean heat content and sea level in 2014–2018. *Science Advances*. 2020 Sep 4;6(36):eabc1151
16. Cao, Dingrui, Kang Xu, Qing-Lan Huang, Chi-Yung Tam, Sheng Chen, Zhuoqi He, and Weiqiang Wang. "Exceptionally prolonged extreme heat waves over South China in early summer 2020: The role of warming in the tropical Indian Ocean." *Atmospheric Research* 278(2022): 106335.
17. Pujiana K, Moum JN, Smyth WD. The role of turbulence in redistributing upper-ocean heat, freshwater, and momentum in response to the MJO in the equatorial Indian Ocean. *Journal of Physical Oceanography*. 2018 Jan 1;48(1):197-220.
18. Pearson, Michael N. *The Indian Ocean*. Routledge, 2003.
19. Schott, F.A., Xie, S.P. and McCreary Jr, J.P., 2009. Indian Ocean circulation and climate variability. *Reviews of Geophysics*, 47(1).
20. Hofmeyr, Isabel. "Universalizing the Indian Ocean." *pmla* 125, no. 3 (2010): 721-729
21. Hofmeyr, I. (2010). Universalizing the Indian Ocean. *pmla*, 125(3), 721-729.
22. Schott, Friedrich A., and Julian P. McCreary Jr. "The monsoon circulation of the Indian Ocean." *Progress in Oceanography* 51, no. 1 (2001): 1-123.

23. Vink, Markus PM. "Indian Ocean studies and the 'new thalassology'." *Journal of Global History* 2, no. 1 (2007): 41-62.

24. Kearney, Milo. *The Indian Ocean in world history*. Routledge, 2004

WEBSITES:

<https://www.britannica.com/place/Pacific-Ocean> accessed on 12th March 2024

<https://www.eea.europa.eu/en/analysis/indicators/chlorophyll-in-transitional-coastal-and#:~:text=Chlorophyll%20is%20an%20indicator,biological%20productivity%20in%20marine%20regions> accessed on 05th December 2023

<https://www.globalchange.gov/browse/indicators/ocean-heat-content-concentrations#:~:text=The%20concentration%20of%20heat%20content%20is,sea%20surface%20temperatures%20and%20winds> accessed on 11th January 2024